Available online at www.sciencedirect.com
SCIENCE DIRECT®
International Journal of Heat and Mass Transfer 47 (2004) 2061–2072
International Journal of HEAT and MASS TRANSFER
www.elsevier.com/locate/ijhmt

Determination of water vapor diffusion and partition coefficients in cement using one FLEC

R. Luo [a,*], J.L. Niu [b]

[a] Department of Thermal Engineering, Tsinghua University, Beijing 100084, PR China
[b] Department of Building Services Engineering, The Hong Kong Polytechnic University, Kowloon, Hong Kong, PR China

Received 29 August 2003; received in revised form 11 December 2003

Abstract

Water vapor diffusion and partition coefficients in cement slabs were determined by solving the inverse problem of one-dimensional unsteady mass diffusion based on measurements of the concentration of water vapor in a field and laboratory emission cell (FLEC) system. A solution for multi-process mass diffusion was obtained to analyze the influence of the non-uniform initial water vapor concentration distribution on the determination of diffusion and partition coefficients. The main factors affecting the accuracy of the diffusion and partition coefficients were discussed. Good agreement between the measured data and the predictions of the inverse problems showed that the mass diffusion in the cement slabs could be described accurately by the one-dimensional model.

Keywords: Mass diffusion; Diffusion coefficient; Partition coefficient; FLEC; Water vapor; Cement

1. Introduction

The determination of heat thermal conductivity and other properties by solving the inverse heat transfer problems has been studied extensively in the past few decades [1–3]. These useful methods and experimental techniques for thermal problems can be applied to the study of inverse mass transfer problems due to their strong similarity to heat transfer problems. Cox et al. [4] estimated the VOC diffusion and partition coefficients by fitting the predicted concentration of the unsteady mass diffusion model to the experimental data on VOC desorption or absorption processes in vinyl. Bodalal et al. [5] determined the VOC diffusion and partition coefficients in building materials by modeling the unsteady VOC diffusion through a slab sealed between two sample chambers.

On other hand, the field and laboratory emission cell (FLEC) has become not only the standard equipment for studying the emission of VOCs from planar building materials [6], but also a potential experimental setup for investigating the mass diffusion process inside solid materials. Since it is difficult, if not impossible, to directly measure the concentration of a substance inside a piece of solid material or on material surface, a FLEC may be the perfect way to obtain the concentration on the emission surface of the solid material by measuring the substance concentration of gas in contact with the surface [7]. Meininghaus and Uhde [8] studied the VOC desorption or absorption and unsteady mass diffusion processes in building materials using two FLEC or one FLEC experimental system.

In the present investigation, the unsteady diffusion processes of water vapor in cement slabs were studied using a one-FLEC system. The diffusion and partition coefficients were determined simultaneously by solving the inverse problem of the unsteady water vapor diffusion in the cement slabs. Unlike conventional applications of FLEC, the water vapor emission surface was a narrow ring, i.e., a partial emission surface in the FLEC, on which a nearly uniform convection mass flux might be achieved. Therefore, the mass diffusion in the test sample may be approximated using a one-dimensional

* Corresponding author. Tel.: +86-10-62782175; fax: +86-10-62772663.
E-mail address: ruiluo@tsinghua.edu.cn (R. Luo).

0017-9310/$ - see front matter © 2003 Elsevier Ltd. All rights reserved.
doi:10.1016/j.ijheatmasstransfer.2003.12.005

Nomenclature

A	emission area (m^2)
Bi_m	mass transfer Biot number
C	concentration (kg/m^3)
D	diffusion coefficient (m^2/s)
F	dimensionless average water content
Fo_m	mass transfer Fourier number
K	partition coefficient
k	convective mass transfer coefficient (m/s)
L	cement ring thickness (m)
M	mass of cement sample
m	total mass transfer
N	number of objective measurement data
q	air flow rate (ml/min)
Re	Reynolds number
RH	relative humidity
r	radial coordinate (m)
Sc	Schmidt number
Sh	Sherwood number
T	temperature (°C) or time constant
t	time
u_m	mean air velocity at the slit (m/s)

Greek symbols

δ	spacing between the emission surface and the cap at air slit (m)
γ	dimensionless concentration
v	kinetic viscosity (m^2/s)

Superscript

$'$	air

Subscripts

a	ambient air
in	inlet of FLEC
m	mean
o	initial
out	outlet of FLEC
s	surface

problem to simplify the analysis. In addition, some factors affecting the determination of diffusion and partition coefficients, particularly the effects of a non-uniform initial distribution of water vapor concentration in cement, were analyzed. Our ultimate goal was to apply the method and technique to investigate the diffusion of VOCs in building materials. Obviously, an investigation of the water vapor diffusion using FLEC with a convenient on-line technique of measuring the moisture content of air is a promising way of approaching the issue.

2. Methodology and experimental apparatus

A cement ring was made by adding water to a mixture of cement and sand and pouring it into a prior machined ring slot on a stainless steel disk. The cement ring in the stainless disk had three surfaces that came into tight contact with the stainless steel, and one surface on the same plane with the disk opening as the emission surface, as shown in Fig. 1. After the cement had dried and aged (about one month) in ambient air, the disk was placed into the low chamber of a FLEC in order to conduct the experiments.

2.1. Air flow loop

Dry synthetic air (with a moisture content of less than 5 ppmv) from a gas cylinder was conditioned in an air supply unit for the desired humidity by letting part of

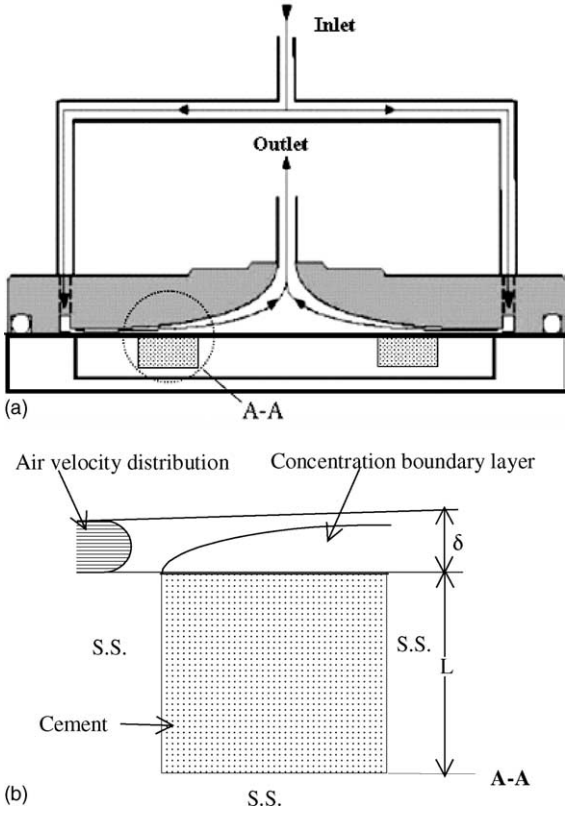

Fig. 1. FLEC (a) and cement sample (b).

the air pass through a water bubbler and then mixing the rest of dry air. The air was then introduced into a FLEC through its inlet, and the air formed a laminar flow in the slit of the FLEC, as shown in Fig. 1. Air was discharged out of the FLEC, after the convective mass transfer process with the cement emission surface was completed.

The rate of air flow into the FLEC was measured and controlled by an air pump before the FLEC inlet. At the same time, a built-in dual temperature–humidity sensor measured the temperature and relative humidity (RH) of inlet air. In a similar way, the temperature and RH of air flow out of the FLEC outlet were monitored by another air pump and built-in sensor of the same type. To maintain the slightly positive pressure in the FLEC to prevent the possible leakage of ambient air into the FLEC, the flow rate of air flowing through the second pump after the outlet was smaller than that flowing into the FLEC. The rest of the air was discharged out of the FLEC under this positive pressure. A more detailed description of the experimental setup can be found in [9].

2.2. Accuracy of the measurements

Since several parameters in the present experiment, such as air flow rate, RH and temperature, might play fundamental roles in determining the diffusion and partition coefficients, the accuracy of the measurement of those parameters is what finally decides the accuracy of the diffusion and partition coefficients. Thus, particular care was taken to calibrate the air flow rate of the pumps and the RH sensors. The accuracy of the measurement of the air flow rate was better than 1%. RH measurements had an uncertainty smaller than 1% over a range of 0–95%. For a low humidity situation of RH = 10–20%, the RH measurement had even better accuracy.

2.3. Determination of the convective mass transfer coefficient

In the same way as described in [9], a water ring made by filling the ring cavity on a plastic plate with water was used as an emission surface for water vapor; i.e., a cement ring was replaced by the water ring with a known RH = 100% on the emission surface. Convective mass transfer was obtained by measuring RH increments of dry synthetic air after the mass transfer had reached steady. A group of water rings with a fixed outside diameter equal to that of the outside diameter of the cement ring, but with different inside diameters was applied to obtain the relationship between the average convective mass transfer coefficient and the inside diameters of the water rings. Finally, the following formula was obtained to estimate the average convective mass transfer coefficient, k,

$$Sh_{\mathrm{m}} = 0.74\,Re^{0.86}\,Sc^{0.68}\left(\frac{r_{\mathrm{o}} - r}{2\delta}\right)^{-0.68}, \tag{1}$$

where

$$Sh_{\mathrm{m}} = \frac{2k\delta}{D'}, \quad Re = \frac{2u_{\mathrm{m}}\delta}{v}, \quad Sc = \frac{v}{D'}. \tag{2}$$

Here, r_{o} and r are the outside and inside diameters of the emission ring, δ is the slit width of the FLEC at a radial position of r, u_{m} is the mean air velocity in the slit, and D' and v are the water vapor diffusion coefficient in air and air kinetic viscosity, respectively.

3. Theory

3.1. One-dimensional unsteady mass diffusion

A cement ring has three surfaces in tight contact with stainless steel, because of the way it has been formed. These three surfaces can be considered as being mass-insulation because of the extremely low diffusion coefficient of water vapor in stainless steel. In addition, a convective mass flux can be considered to be approximately uniformly distributed over the emission surface of the cement ring. Therefore, mass diffusion in the cement ring may be regarded as one-dimensional unsteady diffusion with the third boundary condition on the emission boundary.

The diffusion equation can be written as by assuming the constant diffusion coefficient, D,

$$\frac{\partial C}{\partial t} = D\frac{\partial^2 C}{\partial y^2}, \tag{3}$$

where C is the water vapor concentration in cement (kg/m^3); and t and y are time and the coordinate perpendicular to the emission surface. However, the diffusion coefficient of water vapor in porous material like cement usually is not a constant and depends on the water vapor content because of the non-linearity of water vapor diffusion [10]. D should be considered to be an effective diffusion coefficient, or, an average diffusion coefficient over a definite range of water vapor content [11]. Since VOC content in building material will be much smaller than water vapor concentration in cement, the constant diffusion coefficient assumption may be more suitable to VOC diffusion [12]. The boundary and initial conditions are

$$\left.\frac{\partial C}{\partial y}\right|_{y=0} = 0, \qquad -D\left.\frac{\partial C}{\partial y}\right|_{y=L} = k\,\Delta C', \tag{4}$$

$$C(0, y) = C_{\mathrm{o}}, \tag{5}$$

where L is the thickness of the cement, as shown in Fig. 1(b), and k is the average convective mass transfer coefficient over the emission surface of the cement. $\Delta C' = \frac{\Delta C'_{\text{out}} - \Delta C'_{\text{in}}}{\ln(\Delta C'_{\text{out}}/\Delta C'_{\text{in}})}$ is the log mean concentration difference in air between the emission surface and the bulk air flow with $\Delta C'_{\text{out}} = C'_{\text{s}} - C'_{\text{out}}$ and $\Delta C'_{\text{in}} = C'_{\text{s}} - C'_{\text{in}}$. C'_{out} and C'_{in} are the concentrations of water vapor in air at the entrance and at the existence of the air slit section on the emission surface. And, C'_{s} is the water vapor concentration on the emission surface. Also, they are equal to the concentrations at the outlet and inlet of FLEC. From mass conservation, we have

$$q(C'_{\text{out}} - C'_{\text{in}}) = kA\,\Delta C' \approx kA\left(C'_{\text{s}} - \frac{C'_{\text{out}} + C'_{\text{in}}}{2}\right), \tag{6}$$

where q is the air flow rate and A is the area of the emission surface. To simplify the analysis, the log mean concentration difference can be approximated by the arithmetic mean difference. It should be noted that the ring emission surface also makes this approximation more accurate due to the short concentration boundary layer over the emission surface as shown in Fig. 1.

At the interface between air and cement, the water vapor concentration on two sides is in a local equilibrium. This is described as

$$C_{\text{s}} = KC'_{\text{s}}, \tag{7}$$

where K is the water vapor partition coefficient at the cement–air interface [4,12].

Using $C_{\text{o}} - KC'_{\text{in}} = C_{\text{o}} - C_{\text{in}}$ and L as the characteristic concentration and length, we obtain

$$\frac{\partial \gamma}{\partial Fo_{\text{m}}} = \frac{\partial^2 \gamma}{\partial y^2}, \tag{8}$$

$$\left.\frac{\partial \gamma}{\partial y}\right|_{y=0} = 0, \qquad -\left.\frac{\partial \gamma}{\partial y}\right|_{y=1} = Bi_{\text{m}}\gamma, \tag{9}$$

$$\gamma(0, y) = 1, \tag{10}$$

where

$$\gamma = \frac{C - C_{\text{in}}}{C_{\text{o}} - C_{\text{in}}} = \frac{C' - C'_{\text{in}}}{C'_{\text{o}} - C'_{\text{in}}}, \quad Fo_{\text{m}} = \frac{Dt}{L^2}, \quad Bi_{\text{m}} = \frac{kL}{DK}\frac{1}{\left(1 + \frac{kA}{2q}\right)}. \tag{11}$$

A well-known solution for Eq. (8) and boundary-initial conditions (9) and (10) is

$$\gamma = \sum_{n=1}^{\infty} b_n \cos(\lambda_n y) \mathrm{e}^{(-\lambda_n^2 Fo_{\text{m}})}, \tag{12}$$

where the characteristic values, λ_n, are the positive roots of

$$\lambda_n \tan(\lambda_n) = Bi_{\text{m}} \tag{13}$$

and

$$b_n = \frac{2\sin(\lambda_n)}{\lambda_n + \sin(\lambda_n)\cos(\lambda_n)}. \tag{14}$$

The following relationships can be derived from Eq. (6)

$$C'_{\text{s}} = \frac{1}{1 - \mathrm{e}^{kA/q}}\left(C'_{\text{in}} - C'_{\text{out}}\mathrm{e}^{kA/q}\right), \tag{15}$$

$$\gamma(Fo_{\text{m}}, 1) = \left(\frac{1}{2} + \frac{q}{kA}\right)\frac{C'_{\text{out}} - C'_{\text{in}}}{C'_{\text{o}} - C'_{\text{in}}} = \left(\frac{1}{2} + \frac{q}{kA}\right)\gamma_{\text{out}}. \tag{16}$$

Eq. (15) will be used to obtain the concentration of water vapor on the emission surface from the measured results, γ_{out}, at the inlet and outlet of the FLEC. At $Fo_{\text{m}} = 0$, i.e., $t = 0$, $C'_{\text{o}} = C'_{\text{s}}$. In a similar way, Eq. (16) links the measured results to the concentration on the emission surface.

In addition, integrating Eq. (6) over time for the whole mass transfer process yields the total mass transfer from the cement. Then,

$$m = \int_0^t q(C'_{\text{out}} - C'_{\text{in}})\,\mathrm{d}t = A\int_0^L (C(y,t) - C(y,0))\,\mathrm{d}y \tag{17}$$

generates

$$m = q\sum (C'_{\text{out}} - C'_{\text{in}})_j\,\Delta t_j, \tag{18}$$

$$m = ALK(C'_{\text{s}} - C'_{\text{in}})\left(1 - \sum \frac{b_n}{\lambda_n}\sin\lambda_n \mathrm{e}^{-Fo\,\lambda_n^2}\right) = ALK(C'_{\text{s}} - C'_{\text{in}})(1 - F) \tag{19}$$

Total mass transfer m may be determined experimentally both by measuring the water vapor concentration difference series, $(C'_{\text{out}} - C'_{\text{in}})_j$, in the outlet and inlet of the FLEC using Eq. (18), and by weighing the cement sample before and after a test. As a result, the partition coefficient, K, may be estimated from the total mass transfer m and from the initial water vapor concentration in cement, $C'_{\text{s}} = C'_{\text{o}}$, using Eq. (19).

3.2. Inverse problem of the unsteady mass diffusion

The inverse problem of the unsteady mass diffusion is posed in the following way: for the given test conditions such as the cement geometric dimensions A and L, air flow rate q, and convective mass transfer coefficient k, a pair of the diffusion and partition coefficients D and K will be found to minimize the difference between the solution (12) and a set of measurements γ_j. A widely

used objective function for the difference is the sum of the squared residuals [3]

$$S = \sum_j (\gamma(Fo_{mj}, 1) - \gamma_j)^2. \tag{20}$$

To minimize S requires

$$\frac{\partial S(D, Bi_m)}{\partial D} = \frac{\partial S(D, Bi_m)}{\partial Bi_m} = 0. \tag{21}$$

Here, for simplicity, Bi_m instead of K is used as the second parameter. Substituting Eq. (21) in Eq. (20) yields

$$\sum_j (\gamma(Fo_{mj}, 1) - \gamma_j) \frac{\partial \gamma(Fo_{mj}, 1)}{\partial D} = 0, \tag{22}$$

$$\sum_j (\gamma(Fo_{mj}, 1) - \gamma_j) \frac{\partial \gamma(Fo_{mj}, 1)}{\partial Bi_m} = 0. \tag{23}$$

Eqs. (22) and (23) should be solved by an iteration method because of their non-linearity. The Levenberg–Marquardt Method is used here to obtain the following iterative form [3]

$$\mathbf{P}_{n+1} = \mathbf{P}_n + (\mathbf{J}(\mathbf{P}_n)^T \mathbf{J}(\mathbf{P}_n) + \mu_n \Omega_n)^{-1} \mathbf{J}(\mathbf{P}_n)^T (\boldsymbol{\gamma}(\mathbf{P}_n) - \boldsymbol{\gamma}), \tag{24}$$

where μ_n in association with Ω_n is used to damp numerical oscillations and instabilities. And

$$\mathbf{P}^T = [D, Bi_m], \tag{25}$$

$$\mathbf{J}(\mathbf{P})^T = \begin{bmatrix} \frac{\partial \gamma(Fo_{m1}, 1)}{\partial D}, \ldots, \frac{\partial \gamma(Fo_{mj}, 1)}{\partial D}, \ldots, \frac{\partial \gamma(Fo_{mN}, 1)}{\partial D} \\ \frac{\partial \gamma(Fo_{m1}, 1)}{\partial Bi_m}, \ldots, \frac{\partial \gamma(Fo_{mj}, 1)}{\partial Bi_m}, \ldots, \frac{\partial \gamma(Fo_{mN}, 1)}{\partial Bi_m} \end{bmatrix}, \tag{26}$$

$$(\boldsymbol{\gamma}(\mathbf{P}_n) - \boldsymbol{\gamma})^T = \lfloor (\gamma(Fo_{m1}, 1) - \gamma_1), \ldots, (\gamma(Fo_{mj}, 1) - \gamma_j), \ldots, (\gamma(Fo_{mN}, 1) - \gamma_N) \rfloor, \tag{27}$$

$$\Omega_n = \mathrm{diag}\lfloor \mathbf{J}(\mathbf{P}_n)^T \mathbf{J}(\mathbf{P}_n) \rfloor. \tag{28}$$

For a set of measurements of water vapor concentration in the inlet and outlet of the FLEC, the concentration of water vapor on the emission surface of the cement, $\boldsymbol{\gamma} = \lfloor \gamma_j \rfloor$, can be estimated by Eq. (15). This concentration is then used to determine $\mathbf{P}^T = [D, Bi_m]$ using Eq. (24).

3.3. Multi-process mass diffusion

The initial distribution of water vapor in cement is assumed to be uniform in Section 3.1. However, unlike heat conduction in solids, it is difficult to uniformly distribute water vapor in solids because the mass diffusion coefficient is usually much smaller than thermal diffusivity. Non-uniform initial distribution may result in error determinations of diffusion and partition coefficients.

This problem can be analyzed in a more general way. A non-uniform water vapor distribution results from either short-time water vapor desorption from the emission surface of cement or from absorption. A simple way to achieve a uniform distribution is to seal the emission surface for a long time. In a similar way, a long-time desorption or absorption may also generate a uniform distribution. However, a desorption or absorption process in experimental investigations usually lasts a relatively short time and, more importantly, two processes may be conducted without interruption in some VOC measurement tests [4,13]. Therefore, the influence of non-uniform initial distribution generated from those short-time processes on the determination of diffusion and partition coefficients should be clarified. In addition, it should be known how long it will be necessary to seal the emission surface to obtain a desired uniform distribution.

Consider a mass transfer problem consisting of a few continuous desorption, absorption or sealing processes, which means that the problem has different boundary conditions on the emission surface. The first process is assumed to have a uniform initial distribution and Bi_m. At time $Fo = Fo^{(1)}$, the concentration in the cement is

$$\gamma = \frac{C(Fo_m^{(1)}, y) - C_{in}}{C_o - C_{in}}. \tag{29}$$

A process with the mass Biot number, $Bi_m^{(1)}$, and inlet concentration, $C_{in}^{\prime(1)}$, then starts at this time. It has an initial distribution

$$\gamma_o^{(1)} = \frac{C_{oy}^{(1)} - C_{in}^{(1)}}{C_{os}^{(1)} - C_{in}^{(1)}} = \frac{(C_o - C_{in}) \sum b_n \cos(\lambda_n y) e^{-Fo_m^{(1)} \lambda_n^2} + C_{in} - C_{in}^{(1)}}{(C_o - C_{in}) \sum b_n \cos(\lambda_n) e^{-Fo_m^{(1)} \lambda_n^2} + C_{in} - C_{in}^{(1)}}, \tag{30}$$

where the initial distribution for the second process has been normalized by the difference between the surface concentration, $C_{os}^{(1)}$, at the time $Fo = Fo^{(1)}$ and $C_{in}^{(1)} = KC_{in}^{\prime(1)}$. Based on the initial distribution, the coefficient in Eq. (12) for the second process, $b_n^{(1)}$, is given as

$$b_n^{(1)} = \begin{cases} \dfrac{\frac{\lambda_n^{(1)}}{2\lambda_n^{(1)} + \sin(2\lambda_n^{(1)})} \sum_k \frac{b_k \cos(\lambda_k) \cos(\lambda_n^{(1)}) e^{-Fo_m^{(1)} \lambda_k^2}}{(Bi_m^{(1)2} - Bi_m^2)} + b_n(\lambda_n^{(1)}) c^{(1)}}{\sum b_n \cos(\lambda_n) e^{-Fo_m^{(1)} \lambda_n^2} + c^{(1)}}, & Bi_m^{(1)} \neq Bi_m, \\ b_n \dfrac{(e^{-Fo_m^{(1)} \lambda_n^2} + c^{(1)})}{\sum b_n \cos(\lambda_n) e^{-Fo_m^{(1)} \lambda_n^2} + c^{(1)}}, & Bi_m^{(1)} = Bi_m, \end{cases} \tag{31}$$

where $C_{\text{in}}^{(1)}$ is the inlet concentration in the second process and $b_n(\lambda_n^{(1)})$ is calculated from $\lambda_n^{(1)}$ using Eq. (14), and

$$c^{(1)} = \frac{C_{\text{in}} - C_{\text{in}}^{(1)}}{C_{\text{o}} - C_{\text{in}}}. \tag{32}$$

In a similar way, the initial distribution and the coefficient in Eq. (12) for the following processes can be determined as soon as the boundary conditions and the inlet water vapor concentration are given. This series of solutions was used in the direct problems of mass diffusion in the present study. Its application to the inverse problem is straightforward but requires more computation time for the calculation of $b_n^{(i)}$.

4. Results and discussion

Three cement samples were used to conduct the water vapor desorption and absorption tests. Their dimensions and some properties are given in Table 1. In Table 1, the mass ratio was the weight ratio of cement, sand and water when the cement samples were made. But the water content might change because water tends to form a layer on top of the mixture and to evaporate as the cement and sand become sedimented. The dry weight of a cement ring was obtained under its water content smaller than 10% of saturated water content, usually after the cement ring was baked 48 h at 80 °C.

Two air flow rates, 50 and 100 ml/min, were used in the tests for S2. Only 100 ml/min was used in the other tests. The average convective mass transfer coefficient estimated using Eq. (1) is $k = 0.00108$ (m/s) at $q = 100$ (ml/min) and $k = 0.00058$ (m/s) at $q = 50$ (ml/min) for S1 and S2, and $k = 0.00136$ (m/s) for S3.

4.1. Non-loading tests

Non-loading tests were conducted for each flow rate and inlet humidity condition of air to obtain the dynamic response of the FLEC system without water vapor emissions from the cement samples. All test conditions and procedures were completely the same as those in the real test runs, except that the lower emission chamber of FLEC was replaced by a stainless steel plate. Fig. 2 shows some results of the non-loading tests. The outlet water vapor concentration in non-loading tests can be described as

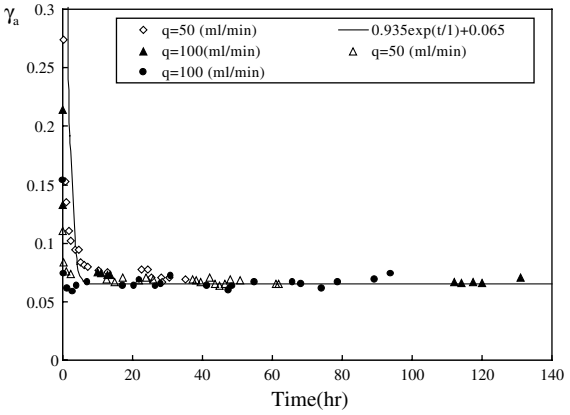

Fig. 2. Non-loading tests and dynamic response of FLEC system. The curve has $T = 1$ h (line).

$$\gamma_{\text{a}} = \frac{C'_{\text{out}} - C'_{\text{in}}}{C'_{\text{a}} - C'_{\text{in}}} = (1-a)\mathrm{e}^{-(t/T)} + a \tag{33}$$

where C'_{a} is the ambient humidity in the lab. Since the FLEC system had some plastic tubes and connections for flexibility, moisture in the atmosphere would diffuse into the system. The first term depends on the volumetric and surface absorption–desorption effects of the FLEC system, and is a short-time term, as shown in Fig. 2. The second term is dependent on the moisture diffusing through the FLEC system from the ambient air, and affects the FLEC system permanently. Thus, the second term must be used to modify the RH measurements of the real tests.

Fig. 2 shows that the FLEC system has an almost stepwise response due to its small volume and low absorption internal surfaces [13]. This means that the water vapor concentrations in air at the local entrance and at the local existence of the air slit section on the emission surface may be represented by those at the RH sensors out of the FLEC without delay. The test results show that a is independent of the air flow rate but slightly dependent on ambient temperature. $a = 0.065$ in the present experiments, which was used to obtain the modification to the measured RH_{out}.

Table 1
Dimensions and properties of samples

Code	Mass ratio cement:sand:water	O.D. $2r_0$ (mm)	I.D. $2r$ (mm)	Thickness L (mm)	Emission area A (cm^2)	Dry weight of cement (g)
S1	2:1:1	115	75	8.5	59.69	100.5
S2	1:1:0.5	115	75	8.8	59.69	104.2
S3	4:1:1	150	130	10	43.98	–

4.2. Determination of diffusion and partition coefficients

A total of 12 test runs were conducted with different flow conditions and inlet humidity to study the main factors affecting the determination of diffusion and partition coefficients. All of the test conditions and important parameters are given in Table 2. RH_{outO} and RH_{outF} are relative humidities in the outlet of the FLEC at the start and the end of the run, respectively. T_a and RH_a are, respectively, the ambient air temperature, i.e., the temperature of the FLEC, and the relative humidity in the lab. ΔRH_a is a modification of the measured RH_{out}, as mentioned in Section 4.1, where $\Delta RH_a = a(RH_a - RH_{in})$. Duration is the length of time of the test run. M_o is the cement mass at the start of the test. m_w is the total mass transfer obtained by weighing the mass difference of the sample before and after the run. m_E is total mass transfer estimated from the sum of all moisture transported by air flow using Eq. (18).

Diffusion and partition coefficients determined from all test runs and other results are given in Table 3. K_1, K_2, and K_3 are the partition coefficients obtained respectively by solving the inverse problem with the method in Section 3.2 and by using weighed and estimated total mass transfer, m, in Eqs. (18) and (19). N is the number of measured data, γ_j, that were used to solve the inverse problem (see Eqs. (26) and (27)). S is the minimum of the sum of the squared errors in Eq. (20).

At the starting stage of each run, the real mass transfer process cannot be described accurately by the one-dimensional mass diffusion, and the initial distribution in cement may be slightly non-uniform. In addition, although the FLEC system has a quick dynamic response as discussed in Section 4.1, the short-time term in Eq. (32) could function even in the first several hours due to the desorption of water vapor absorbed on the surfaces of the FLEC system. Therefore, the measured outlet water vapor concentration at the

Table 2
Test conditions and important parameters

Sample	Run code	q (ml/min)	RH_{in} (%)	RH_{outO} (%)	RH_{outF} (%)	T_a (C)	RH_a (%)	ΔRH_a (%)	Duration (h)	M_o (g)	m_w (g)	m_E (g)
S1	S1D1(14/4)	100	2.0	99.5	19.8	24.2 ± 1	81	5.1	262.9	107.73	6.11	5.91
	S1D2(5/5)	100	1.7	98.0	12.7	25.6 ± 1	70	4.6	166.8	103.38	2.47	2.35
	S1D3(24/5)	100	1.7	81.0	16.8	24.8 ± 1	73	4.6	72.8	102.15	1.40	1.41
	S1A4(26/4)	100	98	18.5	95.0	24.5 ± 1	78	−1.3	215.3	101.60	1.51	1.69
S2	S2D1(28/5)	100	1.8	75.1	8.9	24.9 ± 1	72	4.7	95.9	105.62	0.81	1.08
	S2D2(6/6)	100	1.8	99.0	13.5	26.0 ± 1	76	4.8	93.0	108.80	2.39	2.38
	S2D3(11/6)	50	1.8	41.7	8.3	25.2 ± 1	70	4.6	186.2	106.52	0.77	0.65
	S2D4(7/7)	50	1.5	80.2	10.3	25.5 ± 1	68	4.5	200.1	105.79	2.08	2.13
	S2A5(23/5)	100	76	15.0	73.8	25.1 ± 1	73	−0.1	97.1	104.28	1.33	1.46
	S2A6(20/6)	50	90	22.8	82.8	25.2 ± 1	75	−0.4	170.8	105.13	1.36	1.41
S3	S3D1(2/4)	100	15	66.8	21.3	24.0 ± 1	75	3.8	239.5	–	–	2.68
	S3A2(12/4)	100	96	22.3	92.3	24.1 ± 1	83	−0.8	279.8	–	–	2.74

Table 3
Diffusion and partition coefficients

Sample	Run code	t_i (h)	$D(E-10)$ (m^2/s)	Bi_m	K_1	K_2	K_3	F	N	$(S/N)^{0.5}$
S1	S1D1(14/4)	22.8	0.62	5.01	10059	9811	9490	0.225	31	0.012
	S1D2(5/5)	22.3	0.75	11.35	3663	3551	3379	0.236	14	0.005
	S1D3(24/5)	24.2	0.71	12.31	3565	3821	3844	0.502	12	0.003
	S1A4(26/4)	24.3	0.74	14.81	2834	2583	2891	0.152	30	0.015
S2	S2D1(28/5)	23.5	1.19	10.63	2663	2321	3094	0.294	16	0.004
	S2D2(6/6)	18.6	1.12	9.40	3072	2922	2909	0.331	12	0.004
	S2D3(11/6)	20.3	0.47	9.81	3620	2337	1973	0.386	32	0.010
	S2D4(7/7)	22.2	1.10	5.54	2711	2591	2654	0.198	30	0.012
	S2A5(23/5)	22.9	1.27	7.28	3511	2860	3120	0.299	20	0.020
	S2A6(20/6)	23.0	1.13	5.05	2896	2100	2177	0.192	26	0.014
S3	S3D1(2/4)	22.5	0.86	6.02	9371	–	8912	0.254	33	0.004
	S3A2(12/4)	23.6	0.86	9.51	5950	–	5628	0.152	35	0.012

starting stage was not used as objective measurement data for determining the diffusion and partition coefficients. The data measured after the time, t_i, were used in order to minimize the influence of multi-dimensionality and the non-uniform initial distribution.

4.3. Absorption and desorption

Fig. 3 shows the measured dimensionless difference in concentration of water vapor between the outlet and inlet of the FLEC in the desorption and absorption tests, S1D1, S1D2, S1D3, and S1A4, for sample S1. The lines in Fig. 3 are the predictions of the difference in dimensionless water vapor concentration for the tests according to diffusion and partition coefficients determined by solving the reverse mass diffusion problems.

Usually the diffusion coefficient is dependent on the water vapor content in cement; i.e., it is not a constant due to the non-linearity of water vapor diffusion in porous solids [10,14]. Although desorption tests S1D2 and S1D3 have different initial water vapor concentrations, variations of their measured dimensionless water vapor concentrations versus time almost coincide, and they then have almost the same determined diffusion coefficients of D. However, since the duration of test S1D3 is 72.8 h, the average water content during the measurement of the outlet water vapor concentration to determine the diffusion coefficient is close to that of test S1D2, which has a duration of 166.8 h. So, two tests actually had nearly the same water vapor content when their diffusion coefficients were determined. Thus, it is not surprising to find that the two tests have close diffusion coefficients.

The absorption process, S1A4, also has the same diffusion coefficient, but has a different partition coefficient. This resulted from the so-called adsorption hysteresis, due to the porous structure of cement [15]. An unusual result is that test S1D1 has a very different desorption process compared with S1D2 and S1D3. Its partition coefficient is much larger and the total mass transfer reaches 6 g. This indicates that free water (liquid) existed in the cement sample during test S1D1.

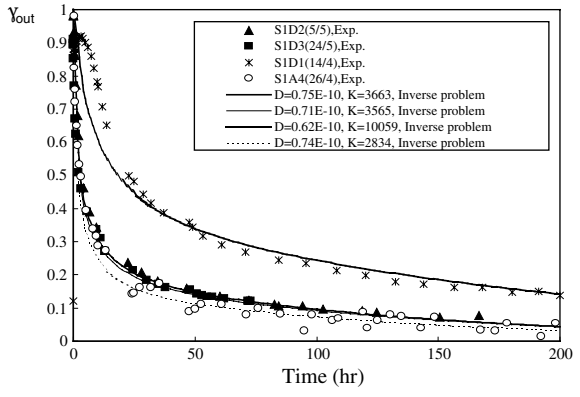

Fig. 3. Water vapor concentration output: Tests and solutions of inverse problems for desorption (S1D1-D3) and absorption (S1A4).

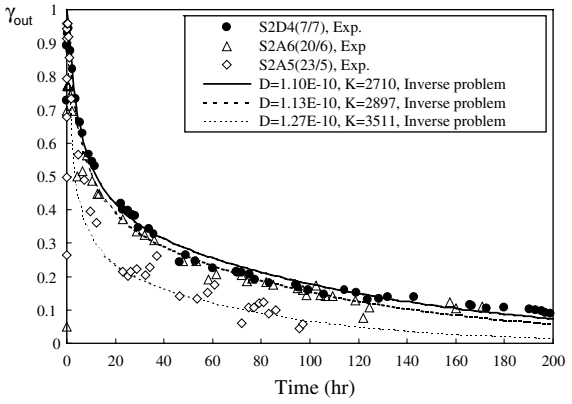

Fig. 4. Tests and solutions of inverse problems for desorption (S2D4) and absorption (S2A5, S2A6).

Fig. 4 shows three test results for sample S2. The most different flow condition is that the air flow rate was 50 ml/min in the two tests, S2D4 and S2A6. For tests at a lower flow rate, the measurements of RH at the outlet of FLEC were susceptible to surrounding conditions. This would result in unstable measured water vapor concentrations. As a result, the minimum of the square-root-mean error, $(S/N)^{0.5}$, is obviously larger than those for the tests at a flow rate of 100 ml/min (see Table 3).

In a similar way, the fluctuation of the measured water vapor concentration in the absorption tests considerably affects the determination of the diffusion and partition coefficients and leads to unreasonable results, particularly for the short duration test, S2A5, as shown in Fig. 4. Indeed, S2A5 has the largest $(S/N)^{0.5}$.

4.4. Effects of non-uniform initial distribution

Fig. 5 shows two tests for S3. An absorption process, S3A2, followed a desorption process, S3D1, without interruption. For this reason, absorption S3A2 appears to have a more obvious hysteresis than S1A4 and S2A6. However, this might result from the effects of non-uniform initial distribution for S3A2. The prediction of a direct problem solution for the desorption–absorption run based on the analysis in Section 3.3 shows that, although the desorption process S3D1 lasted for 239.5 h, the non-uniform water vapor concentration distribution generated by the desorption still affected the absorption process, S3A2, as shown in Fig. 6.

Fig. 6 shows two tests for S2. Both tests S2D1(28/5) and S2D2(6/6) are desorptions. Before S2D2(6/6), sample S2 was sealed for 48 h at temperature of 80 °C for a

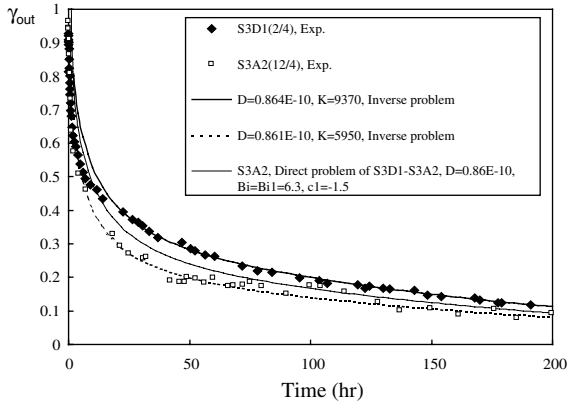

Fig. 5. Desorption and absorption tests and inverse problems and direct problem (thin line) for S3.

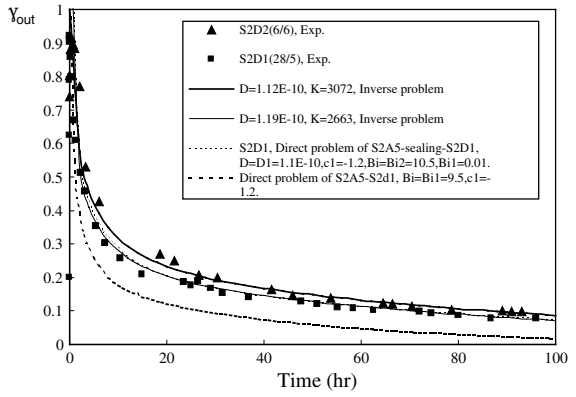

Fig. 6. Tests and inverse problems and direct problems with a 24 h sealing (thin dashed line) or without sealing (thick dashed line) for S2.

better uniform initial distribution of water vapor. Unlike S2D2, S2D1(28/5) was conducted with only a 24 h sealing of S2 at room temperature after the absorption test, S2A5. Fig. 7 later shows that a 24 h sealing at room temperature after an absorption process created a nearly uniform water vapor distribution for cement sample S2, with a relatively large diffusion coefficient. But, there is a noticeable difference between the two desorption tests that might result in a slightly large diffusion coefficient and, in particular, a small partition constant. If a desorption test proceeds immediately after an absorption process (S2A5), it will generate a very different water vapor concentration output from that of a normal desorption with a uniform initial distribution (see the thick dashed line at the bottom of Fig. 6).

Fig. 7 shows the evolution of the water vapor concentration distribution in cement sample S2 during a whole test circulation, consisting of an absorption

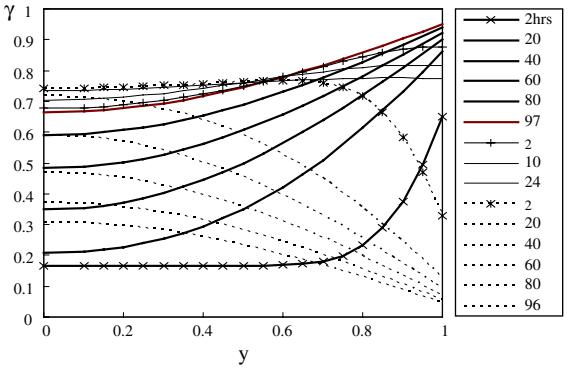

Fig. 7. Evolution of water vapor concentration in cement during an absorption (S2A5, thick solid lines)–sealing (thin solid lines)–desorption (S2D1, thin dash lines) multi-process diffusion.

(S2A5), a sealing (24 h), and a desorption (S2D1). It can be seen that the water vapor concentration peak near the emission surface ($y = 1$) produced during the absorption is damped by the sealing and the desorption. It should be noted that the dimensionless water vapor concentration in Fig. 7, unlike that in Fig. 6, has been normalized with $C_{in} - C_{in}^{(1)} = C_{in} - C_{in}^{(2)}$ to compare three processes according to the same base.

Fig. 8 shows another desorption test for S2, S2D3(11/6). A diffusion coefficient much smaller than those in other tests for S2 was obtained. Since the diffusion coefficient is dependent on average water vapor concentration and very different diffusion coefficients were observed for different concentration diffusions by Garbalinska [11], this result might be partially due to the small average water content. However, an unordinary large initial cement sample weight in S2D3(11/6) indicates that the initial average water content should be

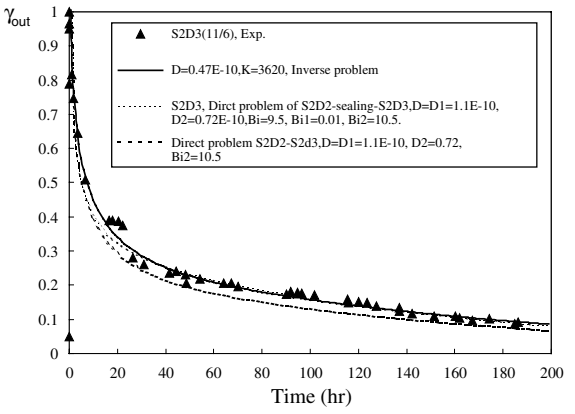

Fig. 8. Test and inverse problem and direct problems with a 26 h sealing (thin dashed line) or without sealing (thick dashed line).

much higher than that presented by its maximum output relative humidity, RH_{OutO}, as shown in Table 3. In a similar way to S2D2(6/6), S2D3(11/6) also followed a 26 h sealing. However, the process before the sealing was S2D2(6/6); i.e., another desorption. Dimensionless water vapor concentration outputs predicted based on the direct problem for the multi-process diffusion, including a desorption S2D2(6/6), a sealing (26 h), and a desorption (S2D3), also are given in Fig. 9. The measured data agree with the prediction for the third process, i.e., desorption S2D2 (11/6) if $D^{(2)} = 0.72\text{E}-10$ (m^2/s), which is considerably larger than that obtained from the inverse problem solution for the data. The evolution of the water vapor concentration in the cement sample, S2, during the multi-process mass diffusion is shown in Fig. 9.

Figs. 7 and 9 show that the water vapor concentration on the emission surface ($y = 1$) changes quickly in the starting stage of a desorption or absorption, while the concentration inside cement is almost not affected. This indicates that the major resistance to the mass transfer is from the mass diffusion process, due to the extremely low water vapor diffusion coefficient in cement. As a result, the water vapor concentration on the emission surface decreases to a very low level after the desorption or absorption process has lasted, say, a quarter or half hour later. Particularly, the surface water vapor concentration will be smaller if the convective mass transfer coefficient may be larger here, e.g. at the leading edge of the concentration boundary layer over the emission surface as shown in Fig. 1(b). Therefore, although the local convective mass transfer coefficient is not uniform on the emission surface as shown by Eq. (1), the mass transfer flux is still approximately uniform owing to the self-adjustment action.

In addition, because the mass diffusion equation with a constant diffusion coefficient, like Eq. (3), is linear, its averaged one-dimensional solution in the y-direction can be obtained by integrating local two- or even three-dimensional solutions over the plane perpendicular to the y-direction, i.e., parallel to the emission surface, if the water vapor concentration distribution is not uniform in the plane. The integration can be performed simply by applying the averaged boundary condition on the whole emission surface. A quite similar but reversely performed approach has been widely used to solve problems of multi-dimensional heat conduction. As we all know, a solution to a multi-dimensional heat conduction problem is a direct product of two or three one-dimensional solutions. Following the same principles, the mass diffusion process in the cement samples could be described accurately using the one-dimensional solution although the mass convection flux on the emission surface may be not strictly uniform.

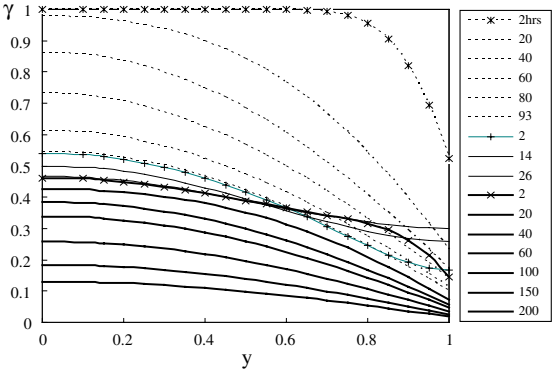

Fig. 9. Evolution of water vapor concentration in cement during a desorption (S2D2, thin dashed lines)–sealing (thin solid lines)–desorption (S2D1, thin solid lines) multi-process diffusion.

It should be noted that the concentration of dimensionless water vapor on the emission surface at the starting stage may be so large that the dimensionless water vapor concentration at the FLEC outlet calculated in Eq. (16) should be over 1. This indicates that the air becomes saturated at the initial emission surface concentration after the air passes through only a part of the emission surface. The mass transfer saturation only happens within a quarter or half hour after the test starts for the present investigation, since the average convective mass transfer coefficient is large due to the small emission area as calculated by Eq. (1).

4.5. Error analysis

One way of analyzing possible errors of determined diffusion and partition coefficients is to study how sensitive the diffusion and partition coefficients are to experimental conditions and to measurements of test parameters. Table 4 gives the changes in the diffusion and partition coefficients for tests S1D2 and S2D4 if one of several parameters or measured data increases by 20%. Here, the number of measured water vapor concentration data used for solving the inverse problems, N, are increased by 3 for both selected tests, which also means a smaller t_i, see Table 3. The t_i for tests S1D2 and S2D4 decreased to 4.2 and 9 h.

Diffusion and partition coefficients are not sensitive to the convective mass transfer coefficient. The determined partition coefficients change considerably if the air flow rate is increased by 20%. However, there is a tiny possibility that a flow rate error of 20% will occur. A similar statement holds for the maximum water vapor concentration difference, $C'_o - C'_{in}$. Errors in the maximum water vapor concentration difference may result from an inaccurate estimate of C'_o in Eq. (15). In addition, a uniformly systematic error in the measurements of water vapor concentration leads to the same influence on the determined diffusion and partition coefficients as $C'_o - C'_{in}$ because the dimensionless water vapor con-

Table 4
Sensitivities of D and K to experimental conditions and measurements of test parameters

Test	Change of D and K	k	q	ΔRH_a	$C'_o - C'_{in}$	N
S1D2(5/5)	$\Delta D/D$	−0.016	0.019	0.178	−0.043	0.005
	$\Delta K/K$	0.003	0.191	−0.126	−0.153	−0.161
S2D4(7/7)	$\Delta D/D$	−0.031	0.036	0.123	−0.090	0.025
	$\Delta K/K$	0.007	0.190	−0.096	−0.149	−0.004

centrations, γ_j, normalized by $C'_o - C'_{in}$ were used as the objective measurement data for the inverse problems.

A larger N means that more data will be used to solve the inverse problem and that the data were those measured in the early stage of the test. If N is small, a few more γ_j measured in the early stage of test may alter the determination of D and K, as seen in test S1D. In contrast, a large N will give rise to more reasonable and unaffected results.

As shown in Table 4, the most serious changes in D and K occur if ΔRH_a increases by 20%. Therefore, the major error may result from the inaccurate measurement of relative humidity in both test runs for D and K or in non-loading runs for the dynamic response of the FLEC system. A non-uniformly systematic error of the measured relative humidity RH in test runs will affect the accuracy of D and K in the same way as the error of ΔRH_a. For a desorption test, RH is usually 10–20% except in the early stage of the test, and ΔRH_a. is around 5%. Thus, 20% of ΔRH_a is about 1%. To make the accuracy of the measurement of RH better than 1% within RH = 10–20%, particular care was paid to the calibrations for the RH sensors. As a result, the diffusion and partition coefficients determined in the present study have an accuracy of better than 15–20%.

To reduce the uncertainty in ΔRH_a, plastic tubes and connections used in the present experiments should be replaced by stainless steel ones for minimum ΔRH_a. If possible, the RH sensors should be mounted directly on the inlet and outlet of the FLEC body.

5. Conclusion

The mass transfer of water vapor in cement was investigated using a one-FLEC system to determine the water vapor diffusion and partition coefficients by solving the inverse unsteady mass diffusion problem. Multi-process mass diffusion problems were also analyzed to study the influence of the non-uniform initial water vapor distributions on the determination of diffusion and partition coefficients. Several conclusions can be drawn as follows:

(1) Although the local convective mass transfer coefficient on the emission surface is not uniform, the unsteady mass diffusion in the cement samples can be described accurately by one-dimensional problems due to the dominant resistance of mass diffusion and the linearity of the mass diffusion equation. Good coincidence between the measured water vapor concentration output and the result predicted by solving the inverse problem of the one-dimensional unsteady mass diffusion supports this statement.
(2) The non-uniform initial water vapor concentration distribution may result in considerable errors in the determined diffusion and partition coefficients. To avoid the errors, the test sample should be sealed for a long time that makes $Fo_m > 1$ for a good uniform initial distribution.
(3) The measurement errors in the relative humidity of air is the major factor affecting the diffusion and partition coefficients. An RH error of 1% might result in errors of 15–20% in the diffusion and partition coefficients. Determined diffusion and partition coefficients for desorption tests have a better accuracy than those for absorption tests.
(4) The FLEC system has a fast dynamic response due to its small volume and internal surfaces of low absorption. The water vapor concentration on the emission surface could be represented without delay by the concentration in the outlet of the FLEC.

Acknowledgements

This research was funded by the PolyU 2000/01 grant for large equipment, and the RGC CERG PolyU 5023/02E. R. Luo was supported by the Croucher Chinese Visitorships of The Croucher Foundation during his visit at BSE of The HK PolyU. The authors appreciate the assistance of technicians Kenny Hung and Wai-Pang Lau of BSE of PolyU in preparing the experimental apparatus.

References

[1] O.M. Alifanov, Inverse Heat Transfer Problems, Springer-Verlag, Berlin, Heidelberg, 1994.
[2] J.V. Beck, B. Blackwell, C.R. St. Clair, Inverse Heat Conduction—Ill-Posed Problem, first ed., Wiley, New York, 1985.

[3] M.N. Ozisik, H.R.B. Orlande, Inverse Heat Transfer—Fundamentals and Applications, Taylor & Francis, 2000.
[4] S.S. Cox, D. Zhao, J.C. Little, Measuring partition and diffusion coefficients for volatile organic compounds in vinyl flooring, Atmospheric Environment 35 (2001) 3823–3830.
[5] A. Bodalal, J.S. Zhang, E.G. Plett, A method for measuring internal diffusion and equilibrium partition coefficients of volatile organic compounds for building materials, Building and Environment 35 (2000) 101–110.
[6] P. Wolkoff, An emission cell for measurement of volatile organic compounds emitted from building materials for indoor use—the field and laboratory emission cell FLEC, Gefahrstoffe Reinhaltung der Luft 56 (1996) 151–157.
[7] F. Haghighat, C.-S. Lee, W.S. Ghaly, Measurement of diffusion coefficients of VOCs for building materials: review and development of a calculation procedure, Indoor Air 12 (2002) 81–91.
[8] R. Meininghaus, E. Uhde, Diffusion studies of VOC mixtures in a building material, Indoor Air 12 (2002) 215–222.
[9] L.Z. Zhang, J.L. Niu, Laminar fluid flow and mass transfer in a standard field and laboratory emission cell, International Journal of Heat and Mass Transfer 46 (2003) 91–100.
[10] P.C. Philippi, H.A. Souza, Modelling moisture distribution and isothermal transfer in a heterogenous porous material, International Journal of Multiphase Flow 21 (1995) 667–691.
[11] H. Garbalinska, Measurement of the mass diffusivity in cement mortar: use of initial rates of water absorption, International Journal of Heat and Mass Transfer 45 (2002) 1353–1357.
[12] X. Yang, Q. Chen, J. Zeng, J.S. Zhang, C.Y. Shaw, A mass transfer model for simulating volatile organic compound emissions from 'wet' coating materials applied to absorptive substrates, International Journal of Heat and Mass Transfer 44 (2001) 1803–1815.
[13] R. Meininghaus, L. Gunnarsen, H.N. Knudsen, Diffusion and sorption of volatile organic compounds in building materials—impact on indoor air quality, Environmental Science and Technology 34 (2000) 3101–3108.
[14] B.X. Wang, Z.H. Fang, Water absorption and measurement of the mass diffusivity in porous media, International Journal of Heat and Mass Transfer 31 (2) (1988) 251–257.
[15] R.J. Murdey, W.D. Machin, Adsorption hysteresis and the pore size distribution of a micro-porous silica gel, Langmuir 10 (1994) 3842–3844.